Redox-Dependent Changes in β-Extended Chain and Turn Structures of Cytochrome *c* in Water Solution Determined by Second Derivative Amide I Infrared Spectra†

Aichun Dong, Ping Huang, and Winslow S. Caughey*

Department of Biochemistry, Colorado State University, Fort Collins, Colorado 80523

Received July 17, 1991; Revised Manuscript Received September 19, 1991

ABSTRACT: The redox-dependent changes in secondary structure of cytochromes *c* from horse, cow, and dog hearts in water at 20 °C have been determined by amide I infrared spectroscopy. Second derivative amide I spectra were obtained by use of a procedure that includes a convenient method for the effective subtraction of the spectrum of water vapor in the system. The band at 1657 cm^{-1} representing the helix structure was unaffected by a change in redox state whereas changes in bands due to turns at 1680, 1672, and 1666 cm^{-1}, unordered structure at 1650 cm^{-1}, and β-structures at 1632 and 1627 cm^{-1} occurred. About one-fourth of the β-extended chain spectral region and one-fifth of the β-turn region (involving a total of approximately 9–13 residues) were sensitive to the oxidation state of heme iron. No significant changes in the secondary structure of either the reduced or oxidized protein due to changes in ionic strength were detected. The localized structural rearrangements triggered by the changes in oxidation state of heme iron are consistent with differences in the binding of heme iron to a histidine imidazole nitrogen and a methionine sulfur atom from the β-extended chain. The demonstrated ability to obtain highly reproducible second derivative amide I infrared spectra confirms the unique utility of such spectral measurements for localization of subtle changes in secondary structure within a protein, especially for changes among the multiple turns and β-structures.

Cytochrome *c* is a small water-soluble protein containing 104 residues in a single polypeptide chain and is one of most throughly studied proteins today in terms of three-dimensional structure (Bushnell et al., 1990; Dickerson et al., 1971; Takano & Dickerson, 1981), structure–function relationships, and physical and chemical properties (Margoliash & Schejter, 1966; Salemme, 1977; Moore et al., 1984; Pielak et al., 1987). It functions as an electron carrier between cytochrome *c* reductase and cytochrome *c* oxidase in the mitochondrial respiratory chain, during which time its heme iron is reversibly oxidized and reduced between the Fe^{2+} and Fe^{3+} oxidation states (Margoliash & Schejter, 1966; Moore et al., 1984). In contrast to many other hemeproteins, the heme moiety of cytochrome *c* is covalently bound to the polypeptide backbone through thioether linkages formed between protoheme IX vinyl groups and two cysteine side chains. In addition, the heme iron forms two coordinate bonds with polypeptide side-chain groups, a histidine imidazole nitrogen and a methionine sulfur atom (Dickerson et al., 1971; Bushnell et al., 1990). The structural flexibility of cytochrome *c* is considered to play a special role in the formation and dissociation of cytochrome *c*/cytochrome *c* reductase and cytochrome *c*/cytochrome *c* oxidase complexes (Margoliash & Schejter, 1966).

Despite the many studies devoted to structure–function relationships in cytochrome *c* (Margoliash & Schejter, 1966; Salemme, 1977; Takano & Dickerson, 1981; Moore et al., 1984; Pielak et al., 1987), the changes in conformation which are concomitant with changes in the oxidation state of heme iron are still under debate. An extensive body of physicochemical data exists which supports some sort of difference in protein structure between the two redox states. Such studies include effects of redox state on the thermal stability (Butt & Keilin, 1962; Margoliash & Schejter, 1966), the molecular compressibility (Eden et al., 1982; Kharakoz & Mkhitaryan, 1986), the susceptibility to proteolytic digestion (Nozaki et al., 1957, 1958), the enthalpy change (Watt & Strutevant, 1969), and the hydrogen–deuterium exchange behavior (Ulmer & Kagi, 1968) as well as antigenic characteristics (Margoliash et al., 1967). These observations have generally been interpreted in terms of different protein conformations in oxidized and reduced species. Circular dichroism (Myer, 1968a,b) and proton NMR spectroscopic studies (Patel & Canuel, 1976; Wand et al., 1986) also support the conclusion that there are two conformations for reduced and oxidized cytochrome *c*. However, these results are in apparent conflict with high-resolution crystallographic studies. Takano and Dickerson (1981a,b) have shown that the crystal structures of the two redox states of tuna cytochrome *c* were essentially the same; it was difficult to identify the differences, and only small atomic displacements were seen when high-resolution maps were compared. The high degree of similarity of the average structure of the two redox forms is also indicated by the extended X-ray absorption fine structure (EXAFS) spectra of horse heart cytochrome *c* (Labhardt & Yuen, 1979) and by comparison of proton paramagnetic NMR shifts of yeast iso-1-cytochrome *c* (Gao et al., 1991). To explain the discrepancies between the crystallographic and other evidence, Eden and co-workers (Eden et al., 1982) proposed that, while the time-averaged structures (as determined by X-ray crystallography) of oxidized and reduced cytochrome *c* are the same, their dynamics are different in that the oxidized form undergoes more low-frequency, large-amplitude motions than the reduced form. Trewhella and co-workers (Trewhella et al., 1988) suggested that the different experimental results may

† This work was supported by U.S. Public Health Service Grant HL-15980 and by Colorado Agricultural Experiment Station Project 643.

* To whom correspondence should be addressed.

0006-2960/92/0431-182$03.00/0

result from protein structural flexibility, which is reflected by changes in structure with changes in ionic strength. Using small-angle X-ray scattering, they found that the radius of gyration and the maximum dimensions of oxidized cytochrome *c* were significantly larger than those for reduced cytochrome *c* in 5 mM phosphate buffer at pH 7.3 and, further, that this difference was suppressed by addition of 200 mM NaCl. Low-salt-dependent structural effects have also been reported in resonance Raman (Liu et al., 1989) and one-dimensional proton NMR studies (Rush et al., 1988). However, the data from a recent two-dimensional proton NMR study does not support this hypothesis (Feng & Englander, 1990).

Infrared spectroscopy is one of the well-established techniques for studying the secondary structures of polypeptides and proteins (Krimm & Bandekar, 1986; Susi & Byler, 1986; Surewicz & Mantsch, 1988). The spectral region most sensitive to protein secondary structural compositions is the so-called amide I band, which is almost entirely due to the C=O stretch vibrations of the peptide linkages and is found from 1700 to 1600 cm^{-1} (Krimm & Bandekar, 1986; Susi & Byler, 1986; Byler & Susi, 1986; Surewicz & Mantsch, 1988). Several methods have been developed to estimate the relative contributions of different types of secondary structures in proteins in solution from their infrared amide spectra: curve-fitting analysis (Byler & Susi, 1986), second derivative analysis (Dong et al., 1990), partial least-squares analysis (Dousseau & Pezolet, 1990), factor analysis (Lee et al., 1990), and data basis analysis (Sarver & Krueger, 1991). Characteristic band frequency assignments of deconvoluted amide I bands for proteins in D_2O as well as in H_2O solutions are now available (Susi & Byler, 1986; Dong et al., 1990). The curve-fitting method is the most utilized procedure in protein infrared studies (Susi et al., 1985; Susi & Byler, 1986; Surewicz et al., 1987; Yang et al., 1987; Arrondo et al., 1988; Holloway & Mantsch, 1989; Cabiaux et al., 1989), but this procedure has several obvious shortcomings. It requires extensive input of band parameters, such as half-bandwidths and band frequencies, in both self-deconvolution and curve-fitting steps, in order to carry out the deconvolution of the protein amide I band contour. The percentages of estimated secondary structures are heavily influenced by the choice of bandwidth and resolution enhancement factor (*K* value) (Cabiaux et al., 1989; Lee et al., 1990). Therefore, the curve-fitting procedure is of limited utility in monitoring rather small alterations in protein conformation. The factor analysis (Lee et al., 1990), partial least-squares analysis (Dousseau & Pezolet, 1990), and data basis analysis (Sarver & Krueger, 1991) procedures have been designed to eliminate the potential bias and uncertainty and to minimize the influence of water absorption by avoiding detailed amide I band deconvolution and band assignments. However, the mathematics of these procedures does not permit detection of the various β-sheets, which are represented by as many as six bands, and of the turn structures, which are represented by up to five bands (Byler & Susi, 1986; Dong et al., 1990). Applications of these methods in supplying the detailed information in protein secondary structures and in monitoring the protein conformational transitions are limited. The infrared second derivative (IR-SD)[1] analysis, on the other hand, deconvolutes the protein amide I band to its components without any parameter input and gives detailed protein secondary structural information (Dong et al., 1990). However, the IR-SD method has been limited by the requirement of a high-quality difference spectrum which, in turn, requires an accurate subtraction of absorptions due to liquid and gaseous water.

We report here an extension of our IR-SD procedure reported earlier (Dong et al., 1990) to monitor any changes in secondary structure of *c*-type cytochromes from three species due to changes in redox state and ionic strength. The highly reproducible spectra obtained made it possible to reliably measure small changes in protein substructures. Significant differences between reduced and oxidized cytochrome *c* were found in β-extended chain and β-turn regions, but no differences in secondary structure occurred from a change in ionic strength. The β-structure rearrangements in cytochrome *c* triggered by the changes in oxidation state indicate that the β-extended chain is an especially flexible portion of the cytochrome *c* molecule.

Materials and Methods

Sample Preparation. Cytochromes *c* from horse heart (type VI), bovine heart (type V), dog heart (type XVIII), lysine (L-5626), and leucine (L-8000) were purchased from Sigma Chemical Co. and used without further purification. Bovine heart cytochrome *c* and dog heart cytochrome *c* were each dissolved in 5 mM sodium phosphate, pH 7.4, to give a 5% (w/v) solution. Horse heart cytochrome *c* was dissolved in 5 mM sodium phosphate, pH 7.4, and also in 5 mM phosphate plus 1 M sodium chloride in each case to give a 5% (w/v) solution. For oxidized cytochrome *c*, a small amount of potassium ferricyanide was added to achieve complete oxidation, followed by passage through a Sephadex G-25 column to remove excess ferricyanide and any reduction products. Reduced cytochrome *c* was obtained by reduction of protein under anaerobic conditions by addition of a small amount of sodium dithionite followed by passage through a Sephadex G-25 column to remove excess dithionite and any oxidation products.

Infrared Spectra Measurements. The protein solutions were prepared for infrared measurement in a Beckman FH-01 cell with CaF_2 windows and a 6-μm path length spacer. Spectra were recorded with a Perkin-Elmer Model 1800 Fourier transform infrared (FT-IR) spectrophotometer at 20 °C following the general procedures reported earlier (Dong et al., 1990). To obtain the spectrum due to protein alone, the spectra due to both liquid water and water vapor were subtracted from the observed spectrum. First, two reference spectra were recorded from the same cell which contained only phosphate buffer by accumulating data twice under conditions identical to those used for the protein solution. For convenience we called these two reference spectra Ref-1 and Ref-2. Since the two reference spectra were identical except for the time-dependent changes in water vapor intensity during continuous purging of the spectrophotometer with dry air, a difference spectrum generated by subtraction of Ref-2 from Ref-1 represented the water vapor spectrum (Figure 1B). Second, a spectrum of the protein solution was recorded using the same cell as used to obtain Ref-1 and Ref-2 after the cell had been vacuum dried.

Difference spectra for proteins were obtained following the criteria described previously (Dong et al., 1990). In the first step, the spectrum of liquid water was subtracted from the observed spectrum of the protein solution to satisfy criterion 2 (a straight base line must be obtained from 2000 to 1700 cm^{-1}), which was achieved by subtracting either Ref-1 or Ref-2 from the spectrum of the protein solution (Figure 1A). In the second step, the water vapor spectrum generated from the difference between Ref-1 and Ref-2 was subtracted from the resultant difference spectrum of step 1 by interactive sub-

[1] Abbreviations: IR-SD, infrared second derivative; FT-IR, Fourier transform infrared.

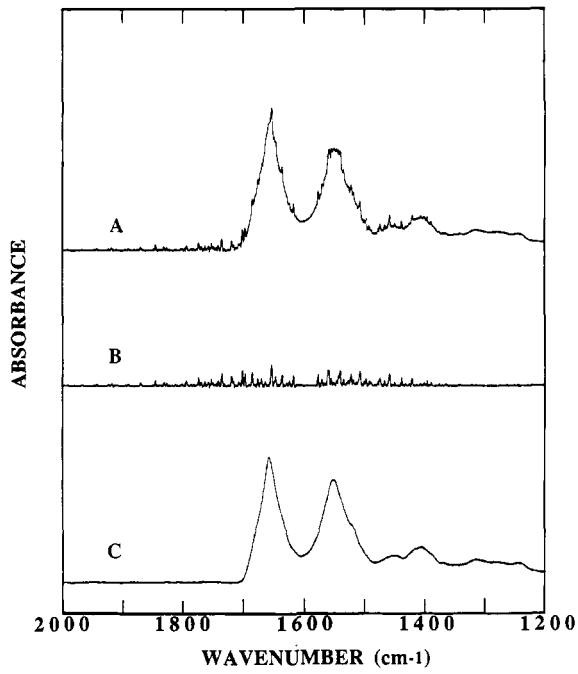

FIGURE 1: Difference spectra of aqueous solutions from 2000 to 1200 cm^{-1} obtained during a double-subtraction analysis of horse heart cytochrome *c*. (A) Difference spectrum of cytochrome *c* obtained from the subtraction of spectrum of Ref-1 from the spectrum of the protein solution; (B) difference spectrum of gaseous water obtained from the subtraction of Ref-2 from Ref-1; and (C) difference spectrum of cytochrome *c* obtained by double subtraction, i.e., spectrum A minus spectrum B.

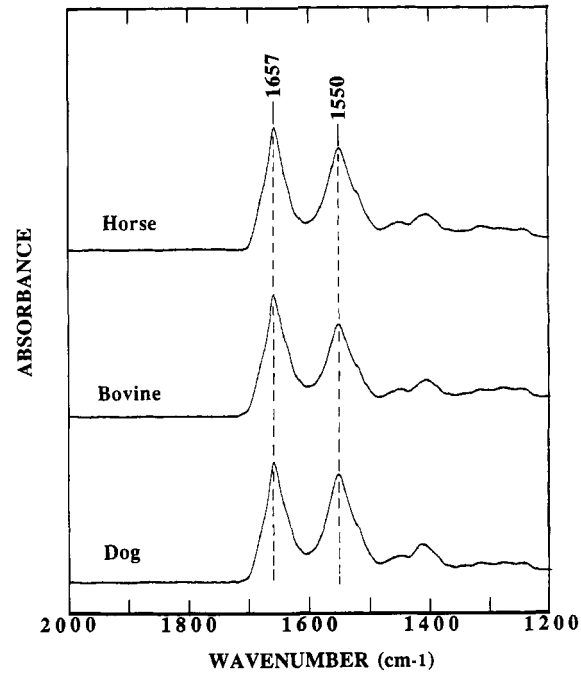

FIGURE 2: Infrared spectra of oxidized cytochromes *c* from horse heart, cow heart, and dog heart (5% w/v) in 5 mM sodium phosphate, pH 7.4, at 20 °C. The amide I, II, and III infrared vibrational bands are observed near 1657, 1550, and 1320–1200 cm^{-1}, respectively.

traction to satisfy criterion 1 (the bands originating from water vapor must be accurately subtracted regardless of the base line) (Figure 1C). The final protein difference spectrum of double subtraction was smoothed with a nine-point Savitsky–Golay function (Savitsky & Golay, 1964) to remove the possible white noise. The second derivative spectrum was obtained with Savitsky–Golay derivative function software for a five data point window. The determination of the relative amounts of different types of secondary structures from the relative intensities of corresponding bands in the second derivative amide I spectrum was performed as described earlier (Dong et al., 1990).

Results

Original Difference Spectra of Cytochrome c. Altogether nine characteristic vibrational bands which arise from the amide groups of polypeptides and proteins have been identified (Krimm & Bandekar, 1986). Among them, the amide I vibrational band, which is due almost entirely to the C=O stretch of the peptide linkages that constitute the backbone structure, is known to be the most sensitive probe of protein secondary structures (Krimm & Bandekar, 1986; Susi & Byler, 1986; Surewicz & Mantsch, 1988). The original difference spectra of oxidized cytochromes *c* from horse heart, bovine heart, and dog heart in 5 mM sodium phosphate, pH 7.4, in the region 2000–1200 cm^{-1} are shown in Figure 2. The spectra conform to the criteria established earlier for subtraction of the spectrum due to liquid and gaseous water from the observed protein spectrum (Dong et al., 1990). The spectra contain bands for amide I (1700–1600 cm^{-1}), amide II (1600–1500 cm^{-1}), and amide III (1320–1200 cm^{-1}). The infrared spectra of oxidized and reduced horse heart cytochrome *c* in 5 mM sodium phosphate plus 1 M sodium chloride solutions were also obtained. At all ionic strength conditions and redox states examined the amide I and amide II band maxima of the cytochromes *c* were observed at 1657 and 1550 cm^{-1}, respectively, which are frequencies that indicate predominantly α-helical character (Koenig & Tabb, 1980; Krimm & Bandekar, 1986).

Second Derivative Amide I Spectra. The amide I band contour consists of a number of individual bands at the frequencies characteristic for specific types of secondary structure (Susi & Byler, 1986; Surewicz & Mantsch, 1988). The second derivative analysis permits the direct separation of the amide I band into its components (Dong et al., 1990). The spectra in Figure 2 represent the amide I bands of horse heart cytochrome *c* in their second derivatives. The secondary structures of two redox states in two ionic strength conditions are compared directly by an overdisplay of second derivative spectra. The high reproducibility of the protein infrared second derivative spectra is clearly indicated by three identical spectra each from a different preparation and measurement under the same redox state and ionic strength conditions. The amide I band frequency assignments for secondary structures in water solution available from previous studies (Gorga et al., 1989; Dong et al., 1990) are as follows: α-helix (1656 ± 2 cm^{-1}), unordered (1650 ± 1 cm^{-1}), β-sheets (multiple bands between 1642 and 1624 cm^{-1}), and turns (multiple bands between 1688 and 1666 cm^{-1}). The quantitative contribution of each type of substructure to the total amide I band contour may be obtained by measuring the integrated band areas assigned to each substructure (Dong et al., 1990). Furthermore, on the basis of the assumption implicit in secondary structure quantitation that the effective intrinsic absorptivities of the amide I bands corresponding to different substructures are essencially the same (Surewicz & Mantsch, 1988), the relative populations can be translated into an approximate number of residues involved in a particular type of secondary structure with the knowledge of the total amino acid residues in the protein.

The most prominent band at 1657 cm^{-1}, which has been assigned to α-helical structure in the second derivative spectra, confirmed the α-helix as the most abundant type of secondary

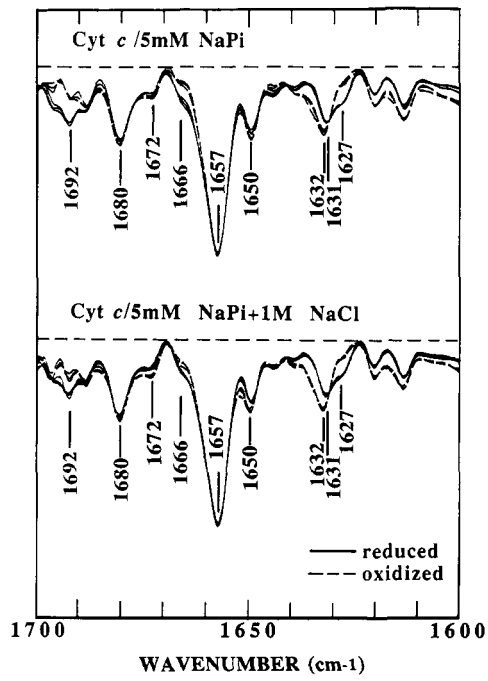

FIGURE 3: Second derivative amide I spectra of oxidized and reduced horse heart cytochrome c in 5 mM sodium phosphate with or without 1 M sodium chloride. (Top panel) Oxidized (---) and reduced (—) cytochromes c in 5 mM sodium phosphate; (bottom panel) oxidized (---) and reduced (—) cytochromes c in 5 mM phosphate plus 1 M sodium chloride. The horizontal dashed lines on the second derivative spectra represent the base line used in quantitating the relative amounts of different types of secondary structures. For each condition, spectra are superimposed for three independent experiments.

structure in aqueous solution. Quantitative evaluations indicate that both reduced and oxidized horse heart cytochromes c consist of 40–42% α-helix, 21–25% β-extended chain, 21–25% β-turns, and 12% unordered structure. These results agree well with the values (45% α-helix, 23% turns) calculated from high-resolution X-ray structure of oxidized horse heart cytochrome c by Bushnell and co-workers (Bushnell et al., 1990). Compared with the β-extended chain region, the α-helices of cytochrome c are more stable and are unaffected by a change in redox state as indicated by the lack of spectral change at the 1657-cm^{-1} band.

Five band frequencies have been assigned to various β-sheet structures, and four of them, the bands at 1642, 1638, 1632, and 1627 cm^{-1}, are commonly found in most β-sheet-containing proteins (Dong et al., 1990). These four common β-sheet bands were also observed in cytochrome c spectra. There was a substantial difference between the second derivative amide I spectra of reduced and oxidized cytochrome c, especially in the region assigned to β-sheet structures. In the oxidized form, the 1632-cm^{-1} band was the single major band due to β-extended chain structure (Dickerson et al., 1971) along with three other minor bands. In the reduced form, there were two major bands at 1631 and 1627 cm^{-1}. Upon reduction the band intensity increased at 1627 cm^{-1} as the 1632-cm^{-1} band weakened, while the band intensities at 1642 and 1638 cm^{-1} remained relatively unchanged. The band intensity ratio of 1632 cm^{-1} to 1627 cm^{-1} was 3.96 ± 0.38 for the oxidized form but only 1.38 ± 0.02 for the reduced form (Table I). Reduction also induced a 1-cm^{-1} red shift of the 1632-cm^{-1} band. These redox-dependent spectral changes were fully reproducible in both low and high ionic strength solutions (Figure 3). The relative band intensity changes suggest that about one-fourth of the β-extended chain residues (approximately 5–7 amino acid residues) are involved in the redox-dependent

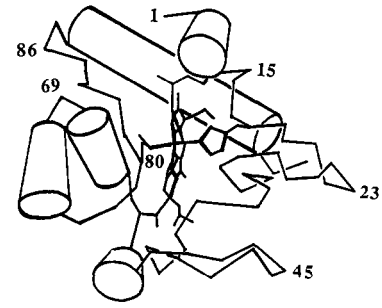

FIGURE 4: Schematic representation of the structure of cytochrome c based on the high-resolution crystal structure of oxidized horse heart cytochrome c (Bushnell et al., 1990). The cylinders represent α-helices.

secondary structure rearrangement. This protein structure rearrangement also involves the neighboring β-turn structure since the redox-dependent infrared spectral changes were found at the region assigned to turn structures. One particular type of β-turn most involved in redox-dependent structural change was represented by the band located at 1666 cm^{-1}. The high-resolution crystallographic study shows that there are six β-turn structures found in the oxidized horse heart cytochrome c: two 3_{10} (type III) turns and four type II turns (Bushnell et al., 1990). Those two 3_{10} turns are located at residues 14–17 and 67–70, respectively, where they make turns to connect the β-extended chains and α-helices (Figure 4). Since the 3_{10} turn resembles one turn of 3_{10} helix, it is expected to show a vibrational band in the amide I infrared region near 1665–1666 cm^{-1} (Krimm & Bandekar, 1986; Yashi et al., 1986). Therefore, we can reasonably assign the 1666-cm^{-1} band, at least in part, to the 3_{10} turn structure. By overlapping the second derivative amide I spectra of reduced and oxidized cytochrome c, it was immediately apparent that the 1666-cm^{-1} band is more intense in the reduced form than in the oxidized one. This 1666-cm^{-1} band intensity increase was at the expense of both the 1680-cm^{-1} band, which can be assigned to type II turns on the basis of the X-ray crystallographic analysis (Bushnell et al., 1990), and the 1672-cm^{-1} band. Quantitative calculation indicated that about one-fifth of the turn structures (approximately 4–6 residues) were involved in the conformational restructuring. Taken together with the changes at the β-extended chain region, the infrared evidence suggests a distinctly different conformation in the reduced cytochrome c compared to that in the oxidized form. Nearly identical redox-dependent protein conformational transitions in terms of secondary structures were also observed in bovine heart cytochrome c and dog heart cytochrome c (Figure 5).

Neither the reduced nor oxidized protein exhibited any secondary structure changes which could be linked to ionic strength variations (Figure 3). The second derivative amide I spectra of horse heart cytochrome c in low and high ionic strength solutions are identical within the same redox state.

It has become clear that some amino acid residue side chains can absorb in the amide I region of the infrared spectrum and should be considered when quantitative estimates of secondary structure composition are calculated (Venyaminov & Kalnin, 1990; Caughey et al., 1991). For protein in H_2O-mediated solutions, the absorptions from side chains of arginine, glutamine, asparagine, and lysine residues have the greatest potential for affecting the secondary structure estimation on the basis of the amide I infrared spectrum (Venyaminov & Kalnin, 1990; Caughey et al., 1991). Among these amino acid residues, lysine is the most likely to influence cytochrome c infrared studies due to the abundance of this group; e.g., horse heart cytochrome c contains 19 Lys, 2 Arg, 3 Gln, and 5 Asn residues (Margoliash & Schejter, 1966). Therefore, as shown

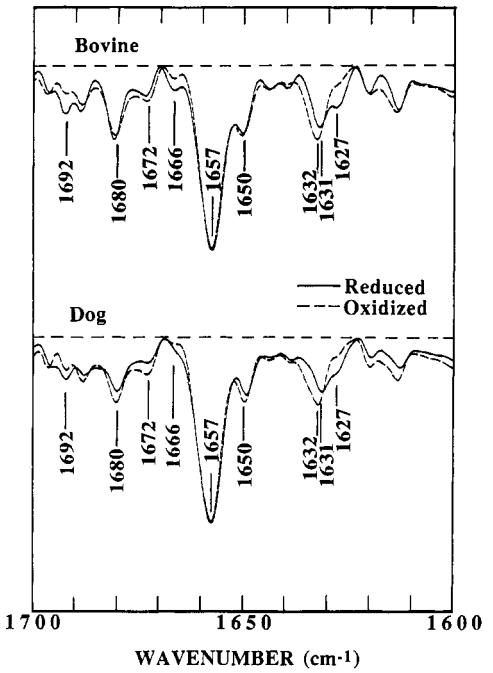

FIGURE 5: Second derivative amide I spectra of cow heart cytochrome *c* and dog heart cytochrome *c* in 5 mM sodium phosphate, pH 7.4. (Top panel) Oxidized (---) and reduced (—) cow heart cytochromes *c*; (bottom panel) oxidized (---) and reduced (—) dog heart cytochromes *c*. The horizontal dashed lines on the second derivative spectra represent the base line used in quantitating the relative amounts of different secondary structures.

in Figure 6, we measured the spectrum of lysine in 50 mM sodium phosphate (pH 7.4). Also shown are the infrared spectrum of leucine, which has a similar side-chain length to lysine, and the difference spectrum generated by subtracting the spectrum of leucine from the spectrum of lysine. The difference spectrum reveals two vibrational bands at 1624 and 1521 cm^{-1} which can be assigned to the asymmetric and the symmetric deformation of ϵ-NH_3^+ group, respectively. However, no band at 1624 cm^{-1} has been found in the second derivative spectra of cytochromes *c* in either "low" or "high" ionic conditions (Figure 3). The side-chain spectral parameters for a residue can be expected to differ somewhat between the free amino acid and the protein microenvironment. Furthermore, the extinction coefficient for the ϵ-NH_3^+ bands is very low. Possibly the ϵ-NH_3^+ group of lysine in cytochrome *c* contributes to the 1620-cm^{-1} band in the second derivative spectra since the formation of a hydrogen or ionic bond between ϵ-NH_3^+ groups and other side-chain groups could result in a band shift to lower wavenumber. It should be pointed out that in a recent study by Venyaminov and Kalnin (1990), an infrared spectrum of lysine side chain was generated by subtracting the spectrum of alanine from the spectrum of lysine at pH 5.6, in which two bands at 1630 and 1526 cm^{-1} were revealed. It is very unlikely that the 1632(1)-cm^{-1} band in the second derivative spectra of cytochromes *c* could arise from a lysine side chain for two obvious reasons. First, the 21–25% of the β-extended chain estimated for the cytochrome *c* on the basis of the second derivative amide I infrared spectra agrees well with the value calculated by Levitt and Greer (1977) on the basis of the X-ray crystallographic analysis. Second, the redox-dependent changes are associated with 1632(1)-cm^{-1} band. The 1629 ± 1 cm^{-1} band for the ϵ-NH_3^+ group obtained from subtraction of alanine from lysine or from dodecylamine by Venyaminov and Kalnin may have resulted from the carbon side-chain differences. Effects of side chains from arginine, glutamine, and asparagine on the amide I infrared spectrum were not considered in the present study due to the low contents of these residues in cytochromes *c*.

Discussion

Redox-Dependent Conformational Transitions of Cytochrome c. In its function as an electron carrier cytochrome *c* cycles between its reductase and oxidase, and certain conformational changes between redox states have been expected to play a role during this process (Margoliash & Schejter, 1966). Recent circular dichroism, magnetic circular dichroism, and resonance Raman experiments have revealed spectral changes in cytochrome *c* after binding to cytochrome *c* oxidase (Weber et al., 1987; Hildebrandt et al., 1990). From an X-ray crystallographic study, Dickerson and co-workers (Deckerson et al., 1971) have shown that the heme group of cytochrome *c* sits in a crevice, with cysteines 14 and 17 and histidine 18 connected to the right wall of the crevice and methione 80, the sixth iron ligand, extending from the left wall as shown in Figure 4. On the right side of the molecule, most of the peptide backbone is best described as extended chain, and on the left side, the secondary structure bonds to the heme iron via the sulfur atom of methione 80 which is also in a β-extended chain (Dickerson et al., 1971). It should be pointed out that a somewhat different description of these β-extended chain regions has been given by Bushnell et al. (1990) in a recent high-resolution X-ray crystallographic study. They described these regions as a random coil structure except for a very short two-stranded antiparallel β-sheet at residues 37–40 and 57–59. However, evidence from several infrared studies (Susi & Byler, 1986; Dong et al., 1990) supports the description of β-extended chain given by Dickerson et al. (1971). By examining the isotropic termperature factors, Takano and Dickerson (1981a) found substantial differences in main-chain flexibility among various substructure regions: the most flexible region is between residues 20 and 28, the so-called extended-chain loop, and the most rigid structures are the α-helices. The atomic mobility map of reduced tuna cytochrome *c* generated by computer dynamic simulation methods agrees with X-ray analysis (Northrup et al., 1980a,b). Our results also support main-chain flexibility among certain secondary structures within the cytochrome *c* molecule. It is not surprising that the above-mentioned extended-chain loops undergo some conformational rearrangements upon redox-state change as indicted by the infrared spectra; the rearrangements in the β-extended chain region are expected to reflect the importance of iron oxidation state on the bonding of heme iron to histidine imidazole nitrogen and to methionine sulfur on the β-structure. The spectra are also consistent with the β-extended chain region being the most flexible substructure in the protein. Liu et al. (1989) examined ultraviolet resonance Raman spectra of horse heart cytochrome *c* in neutral solution at ionic strengths of 5 mM and 1.5 M and found that the α-helical content was not influenced by the redox state and ionic strength changes. However, Feng and Englander (1990), by comparing the chemical shift of reduced and oxidized cytochromes *c* in both "low" (5 mM phosphate) and "high" (5 mM phosphate plus 200 mM NaCl) ionic strength conditions by two-dimensional proton NMR spectroscopy, found substantial discrepancies between the two redox forms. The differences were mainly concentrated in the region involving residues 39–43 and 50–60 as well as some discontinuous residues near both heme ligands. The results of Feng and Englander suggest that both β-extended chain and α-helix may be involved in redox-dependent structure changes, whereas our findings revealed no changes in α-helical structure region. The two studies do both support no sizable protein structure

Table I: Relative Band Intensities in Second Derivative Amide I Infrared Spectra of Horse Heart Cytochrome c in 5 mM Sodium Phosphate, pH 7.4, at 20 °C

	band intensity ratio ± SD			
redox state	1632(1) cm^{-1}/1627 cm^{-1}	1657 cm^{-1}/1666 cm^{-1}	1657 cm^{-1}/1632-(1) cm^{-1}	1657 cm^{-1}/1627 cm^{-1}
reduced	1.38 ± 0.02	5.67 ± 0.36	3.55 ± 0.07	5.17 ± 0.06
oxidized	3.96 ± 0.38	12.17 ± 0.13	3.00 ± 0.13	11.17 ± 0.56

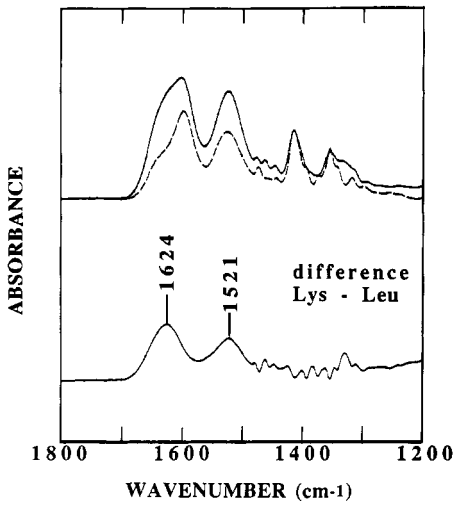

FIGURE 6: Infrared spectra of lysine and leucine in 50 mM sodium phosphate (pH 7.4) at 20 °C, and the lysine minus leucine difference spectrum. The spectra of lysine (—) and leucine (---) were measured under the same scan conditions as used for cytochromes c.

changes linked to ionic strength changes. However, it must be recognized that utilizing the amide I infrared spectra to detect conformational transitions in proteins is limited to the changes involving secondary structures; therefore, changes in tertiary structure may not be reflected in the amide I infrared spectra. Thus the lack of spectral differences in amide I infrared spectra of cytochrome c between low and high ionic strength conditions cannot completely rule out possible changes in tertiary structure. Since the X-ray-derived structures for the Fe^{2+} and Fe^{3+} proteins show no apparent conformational difference (Takano & Dickerson, 1981a,b), there is inconsistency between our infrared findings and those from X-ray crystallography. The general similarity of solution and crystal structures is supported by infrared spectra for many proteins (Susi & Byler, 1986; Dong et al., 1990). However, the assumption that crystal and solution structures are identical in all respects is not warranted. For example, distinct differences between crystal and solution structures are found for hemoglobin (Potter et al., 1985) and myoglobin (Makinen et al., 1979) carbonyls. By comparison of proton paramagnetic NMR shifts in reduced and oxidized yeast C102T iso-1-cytochrome c, Gao et al. (1991) concluded that there are no major conformational changes upon changing the oxidation state of cytochrome c in solution. However, these authors noted differences between computed dipolar shifts based on crystallographic data and observed dipolar shifts deduced from their NMR data. These differences occurred in regions near residues 14–19, 30–43, 53–59, and 79–82, especially at residue 41. These residues are those involved in most of the β-extended chain and turns. However, it was not clear whether the differences had their origin in redox- or crystal–solution-dependent changes, or both. Our infrared results show 9–13 residues are involved in the redox-dependent structural change with 4–6 in the turn region and 5–7 in the β-extended chain region.

Handling Water Absorptions by Double Subtraction. Infrared spectroscopy constituted one of the earliest experimental methods for studying protein secondary structures (Elliott & Ambrose, 1950). The development of computerized FT-IR instrumentation along with the use of short path length cells (~6–10 μm) permitted reliable subtraction of the water spectrum (Koenig & Tabb, 1980; Dong et al., 1990). Nevertheless, infrared studies on protein secondary structure have been almost entirely limited to solid-state preparations (Parker, 1983) and deuterium oxide solutions (Yang et al., 1985; Byler & Susi, 1986; Casal et al., 1988; Holloway & Mantsch, 1988; Perkins et al., 1989; Prestrelski et al., 1991) due to the interference of water absorption in the amide I region. There are two sources of water absorption which severely interfere with the infrared protein amide I band analysis: liquid water and gaseous water (Dong et al., 1990). Over the past decade, attention has been mainly focused on the subtraction of the spectrum of lipid water from the observed spectrum of protein solutions (Koenig & Tabb, 1980; Haris et al., 1986; Powell et al., 1986; Dousseau et al., 1989; Dong et al., 1990). Two least-square algorithm procedures have been developed for this purpose (Powell et al., 1986; Dousseau et al., 1989). The subtraction of gaseous water, the most important factor leading to formation of artificial band(s) upon self-deconvolution or second derivative analysis (Mantsch et al., 1989; Lee et al., 1990), from the observed spectrum of protein solution has not been studied in detail. In our earlier report (Dong et al., 1990), we established two criteria for obtaining successful water subtraction. Criterion 1 (the bands originating from water vapor must be accurately subtracted regardless of the base line) deals mainly with the subtraction of the gaseous water spectrum, and criterion 2 (a straight base line must be obtained from 2000 to 1700 cm^{-1}) deals primarily with the subtraction of the liquid water spectrum. However, since the infrared band intensities of gaseous water are continuously changing during the course of the experiment due to changes in the effectiveness of dry air purging, satisfying both criterion 1 and criterion 2 in one single step of water subtraction proves to be difficult to achieve in practice. On the other hand, the double-subtraction procedure described above has been found to enable both criteria to be satisfied easily and to result in a highly accurate difference spectrum which, in turn, makes achievement of highly reproducible second derivative analyses possible (Figure 3). The application of the double-subtraction procedure is not limited only to protein amide I band analysis but is applicable to any region of the infrared spectrum where interference of gaseous water may become a major problem.

Conclusions. A convenient and effective procedure for the subtraction of liquid and gaseous water spectra was described. The highly reproducible amide I spectrum obtained following subtraction of the water spectra was found to permit a detailed IR-SD analysis of subtle changes in the secondary structure of proteins in water solution. The second derivative amide I infrared spectra of cytochromes c from horse, cow, and dog hearts gave direct evidence of substantial differences between the secondary structures of the reduced and oxidized states. The structural differences were mainly localized at the region of β-extended chain and the connecting turn structures consistent with the most flexible structure in cytochrome c being the β-extended chain region. Alterations in secondary structure due to changes in ionic strength were not found. The close relationship between protein conformation and redox state of the heme iron in cytochrome c is expected to be an important determinant in cytochrome c function during reactions with cytochrome c oxidase and cytochrome c reductase. These

results demonstrate the ability of the IR-SD method used to readily detect subtle shifts in secondary structure at 9–13 out of 104 amino acid residues with some of the changes in the spectrum almost certainly due to a change at a single amino acid residue.

ACKNOWLEDGMENTS

We thank Dr. Byron W. Caughey for critical review of the manuscript.

Registry No. Cytochrome *c*, 9007-43-6; iron, 7439-89-6; heme, 14875-96-8.

REFERENCES

Arrondo, J. L. R., Young, N. M., & Mantsch, H. H. (1988) *Biochim. Biophys. Acta 952*, 261–268.

Bushnell, G. W., Louie, G. V., & Brayer, G. D. (1990) *J. Mol. Biol. 214*, 585–595.

Butt, W. D., & Keilin, D. (1962) *Proc. R. Soc. London, B 156*, 429–458.

Byler, D. M., & Susi, H. (1986) *Biopolymers 25*, 469–487.

Cabiaux, V., Goormaghtigh, E., Wattiez, R., Falmagne, P., & Ruysschaert, J.-M. (1989) *Biochimie 76*, 153–158.

Casal, H. L., Korich, U., & Mantsch, H. H. (1988) *Biochim. Biophys. Acta 957*, 11–20.

Caughey, B. W., Dong, A., Bhat, K. S., Ernst, D., Hayes, S. F., & Caughey, W. S. (1991) *Biochemistry 30*, 7672–7680.

Dickerson, R. E., Takano, T., Eisenberg, D., Kallai, O. B., Samson, L., Cooper, A., & Margoliash E. (1971) *J. Biol. Chem. 246*, 1511–1535.

Dong, A., Huang, P., & Caughey, W. S. (1990) *Biochemistry 29*, 3303–3308.

Dousseau, F., & Pezolet, M. (1990) *Biochemistry 29*, 8771–8779.

Dousseau, F., Therrien, M., & Pezolet, M. (1989) *Appl. Spectrosc. 43*, 538–542.

Eden, D., Matthew, J. B., Rosa, J. J., & Richards, F. M. (1982) *Proc. Natl. Acad. Sci. U.S.A. 79*, 815–819.

Elliott, A., & Ambrose, E. J. (1950) *Nature 165*, 921–922.

Feng, Y.-Q., & Englander, S. W. (1990) *Biochemistry 29*, 3505–3509.

Gao, Y., Lee, A. D. J., Williams, R. J. P., & Williams, G. (1989) *Eur. J. Biochem. 182*, 57–65.

Gao, Y., Boyd, J., Pielak, G. J., & Williams, R. J. P. (1991) *Biochemistry 30*, 1928–1934.

Gorga, J. C., Dong, A., Manning, M. C., Woody, R. W., Caughey, W. S., & Strominger, J. L. (1989) *Proc. Natl. Acad. Sci. U.S.A. 86*, 2321–2325.

Haris, P. I., Lee, D. C., & Chapman, D. (1986) *Biochim. Biophys. Acta 874*, 255–265.

Hildebrandt, P., Heimburg, T., Martsh, D., & Powell, G. J. (1990) *Biochemistry 29*, 1661–1668.

Holloway, P. W., & Mantsch, H. H. (1988) *Biochemistry 27*, 7991–7993.

Holloway, P. W., & Mantsch, H. H. (1989) *Biochemistry 28*, 931–935.

Kharakoz, D. P., & Mkhitaryan, A. G. (1986) *Mol. Biol. 20*, 312.

Koenig, J. L., & Tabb, D. L. (1980) in *Analytical Application of FT-IR to Molecular and Biological Systems* (During, J. R., Ed.) pp 241–255, D. Reidel Publishing Co., Dordrecht.

Krimm, S., & Bandekar, J. (1986) *Adv. Protein Chem. 38*, 181–364.

Labhardt, A., & Yuen, C. (1979) *Nature 277*, 150–151.

Lee, D. C., Haris, P. I., Chapman, D., & Mitchell, R. C. (1990) *Biochemistry 29*, 9185–9193.

Levitt, M., & Greer, J. (1977) *J. Mol. Biol. 114*, 181–293.

Liu, G.-Y., Grygon, C. A., & Spiro, T. G. (1989) *Biochemistry 28*, 5046–5050.

Makinen, M. W., Houtchens, R. A., & Caughey, W. S. (1979) *Proc. Natl. Acad. Sci. U.S.A. 76*, 6042–6046.

Mantsch, H. H., Surewicz, W. K., Muga, A., Moffatt, D. J., & Casal, H. L. (1989) *7th International Conference on Fourier Transform Spectroscopy, Fairfax, VA 1989* (Cameron, D. G., Ed.) Proc. SPIE—Int. Soc. Opt. Eng. 1145, pp 580–581, SPIE, Bellingham, WA.

Margoliash, E., & Schejter, A. (1966) *Adv. Protein Chem. 21*, 113–286.

Margoliash, E., Reichlin, M., & Nisonoff, A. (1967) *Science 158*, 531.

Moore, G. R., Eley, C. G. S., & Williams, G. (1984) *Adv. Inorg. Bioinorg. Mech. 3*, 1–96.

Myer, Y. P. (1968a) *Biochemistry 7*, 765–776.

Myer, Y. P. (1968b) *J. Biol. Chem. 243*, 2115–2122.

Northrup, S. H., Pear, M. R., McCammon, J. A., & Karplus, M. (1980a) *Nature 286*, 304–305.

Northrup, S. H., Pear, M. R., McCammon, J. A., Karplus, M., & Takano, T. (1980b) *Nature 287*, 659–660.

Nozaki, M., Yamanaka, T., Horio, T., & Okunuki, K. (1957) *J. Biochem. 44*, 453–464.

Nozaki, M., Yamanaka, T., Horio, T., & Okunuki, K. (1958) *J. Biochem. 5*, 815–823.

Parker, F. S. (1983) *Applications of Infrared, Raman and Resonance Raman Spectroscopy in Biochemistry*, Plenum Press, New York.

Patel, D. J., & Canuel, L. L. (1976) *Proc. Natl. Acad. Sci. U.S.A. 73*, 1398–1402.

Perkins, S. J., Nealis, A. S., Haris, P. I., Chapman, D., Goundis, D., & Reid, K. B. M. (1989) *Biochemistry 28*, 7176–7182.

Pielak, G. J., Concar, D. W., Moore, G. R., & Williams, R. J. P. (1987) *Protein Eng. 1*, 83–88.

Potter, W. T., Houtchens, R. A., & Caughey, W. S. (1985) *J. Am. Chem. Soc. 107*, 3350–3352.

Powell, J. R., Wasacz, F. M., & Jakosen, R. J. (1986) *Appl. Spectrosc. 40*, 339–344.

Prestrelski, S. J., Byler, D. M., & Liebman, M. N. (1991) *Biochemistry 30*, 133–143.

Rush, J. D., Koppenol, W. H., Garber, E. E., & Margoliash, E. (1988) *J. Biol. Chem. 263*, 7514–7520.

Salemme, F. R. (1977) *Annu. Rev. Biochem. 46*, 299–329.

Sarver, R. W., & Krueger, W. C. (1991) *Anal. Biochem. 194*, 89–100.

Savitsky, A., & Golay, J. E. (1964) *Anal. Chem. 36*, 1628–1639.

Surewicz, W. K., & Mantsch, H. H. (1988) *Biochim. Biophys. Acta 952*, 115–130.

Surewicz, W. K., Moscarello, M. A., & Mantsch, H. H. (1987) *J. Biol. Chem. 262*, 8598–8602.

Susi, H., & Byler, D. M. (1986) *Methods Enzymol. 130*, 290–311.

Susi, H., Byler, D. M., & Purcell, S. M. (1985) *J. Biochem. Biophys. Methods 11*, 235–240.

Takano, T., & Dickerson, R. E. (1981a) *J. Mol. Biol. 153*, 79–94.
Takano, T., & Dickerson, R. E. (1981b) *J. Mol. Biol. 153*, 95–115.
Trewhella, J., Carlson, V. A. P., Curtis, E. H., & Heidorn, D. B. (1988) *Biochemistry 227*, 1121–1125.
Ulmer, D. D., & Kagi, J. H. R. (1968) *Biochemistry 7*, 2710–2717.
Venyaminov, S. Y., & Kalnin, N. N. (1990) *Biopolymers 30*, 1243–1257.
Wand, J. A., Rober, H., & Englander, S. W. (1986) *Biochemistry 25*, 1107–1114.
Watt, G. D., & Sturtevant, J. M. (1969) *Biochemistry 8*, 4567–4571.
Weber, C., Michel, B., & Bosshard, H. R. (1987) *Proc. Natl. Acad. Sci. U.S.A. 84*, 6687–6691.
Yang, P. W., Mantsch, H. H., Arrondo, J. L. R., Saint-Girons, I., Guillou, Y., Cohen, G. N., & Barzu, O. (1987) *Biochemistry 26*, 2706–2711.
Yang, W.-J., Griffiths, P. R., Byler, D. M., & Susi, H. (1985) *Appl. Spectrosc. 39*, 282–287.
Yashi, S. C., Keiderling, T. A., Bonora, G. M., & Toniolo, C. C. (1986) *Biopolymers 25*, 79–89.

Electron Spin Echo Envelope Modulation Spectroscopic Study of Iron–Nitrogen Interactions in Myoglobin Hydroxide and Fe(III) Tetraphenylporphyrin Models†

Richard S. Magliozzo*,‡ and Jack Peisach‡,§

Department of Molecular Pharmacology and Department of Physiology and Biophysics, Albert Einstein College of Medicine of Yeshiva University, Bronx, New York 10461

Received June 17, 1991; Revised Manuscript Received September 26, 1991

ABSTRACT: The electron–nuclear coupling in low-spin iron complexes including myoglobin hydroxide (MbOH) and two related model compounds, Fe(III) tetraphenylporphyrin(pyridine)(OR^-) (R = H or CH_3) and Fe(III) tetraphenylporphyrin(butylamine)(OR^-) was investigated using electron spin echo envelope modulation (ESEEM) spectroscopy. The assignment of frequency components in ESEEM spectra was accomplished through the use of nitrogen isotopic substitution wherever necessary. For example, the proximal imidazole coupling in MbOH was investigated without interference from the contributions of porphyrin ^{14}N nuclei after substitution of the heme in native Mb with ^{15}N-labeled heme. Computer simulation of spectra using angle selected techniques enabled the assignment of parameters describing the hyperfine and quadrupole interactions for axially bound nitrogen of imidazole in MbOH, of axial pyridine and butylamine in the models, and for the porphyrin nitrogens of the heme in native MbOH. The isotropic component of axial nitrogen hyperfine interactions exhibits a trend from 5 to 4 MHz, with imidazole (MbOH) > pyridine > amine. The nuclear quadrupole interaction coupling constant e^2Qq was near 2 MHz for all nitrogens in these complexes. The Q_{zz} axis of the nuclear quadrupole interaction tensor for the proximal imidazole nitrogen in MbOH was found to be aligned near g_z (g_{max}) in MbOH, suggesting that g_z is near the heme normal. A crystal field analysis, that allows a calculation of rhombic and axial splittings for the d orbitals of the t_{2g} set in a low-spin heme complex, based on the g tensor assignment $g_z > g_y > g_x$, yielded results that are consistent with the poor π-acceptor properties expected for the closed shell oxygen atom of the hydroxide ligand in MbOH. A discussion is presented of the unusual results reported in a linear electric field effect in EPR (LEFE) study of MbOH published previously [Mims, W. B., & Peisach, J. (1976) *J. Chem. Phys. 64*, 1074–1091].

An understanding of the chemistry of the prosthetic group and its axial ligands in heme proteins has often been provided by magnetic resonance spectroscopic studies. For example, ESEEM[1] spectroscopy, a pulsed EPR technique that directly probes the interactions between unpaired electrons and nearby nuclei of ^{14}N-containing ligands has been used to study the axial ligation in various low-spin heme protein complexes (Peisach et al., 1979; Magliozzo et al., 1987). The approach to this type of investigation involved comparisons between protein and iron porphyrin or heme model complexes, a technique that remains especially useful because models containing different axial ligands can be readily prepared. A complete quantitative analysis of the electron–nuclear couplings in some of those systems, however, was not possible because of the need to simultaneously assign parameters, including those for the nuclear Zeeman, hyperfine, and quadrupole interactions, for both axial and equatorial ligand nitrogens. A method involving isotopic substitution can sometimes be used to assign the spectral contributions of the various ligands. For example, substitution of ^{15}N for ^{14}N in the histidines of yeast cytochrome *c* oxidase (Martin et al., 1985) was used to simplify the spectra in an ENDOR study to identify the axial ligands to the heme. Isotopic substitution of the native prosthetic group in a heme protein by recon-

† This work was supported by Grants GM-40168 and RR-02583 from the National Institutes of Health.
* Author to whom correspondence should be addressed.
‡ Department of Molecular Pharmacology.
§ Department of Physiology and Biophysics.

[1] Abbreviations: ESEEM, electron spin echo envelope modulation; ENDOR, electron–nuclear double resonance; TPP, tetraphenylporphyrin; Hb, hemoglobin, Mb, myoglobin; LEFE, linear electric field effect; nqi, nuclear quadrupole interaction; nqr, nuclear quadrupole resonance; pyr, pyridine.

0006-2960/92/0431-189$03.00/0